Astron. Astrophys. 357, 359–366 (2000)

ASTRONOMY AND ASTROPHYSICS

CO emission mechanisms in C/1995 O1 (Hale-Bopp)

M.T. Capria, A. Coradini, M.C. De Sanctis, and R. Orosei

Istituto di Astrofisica Spaziale (IAS), CNR, Area di Ricerca di Tor Vergata, Via del Fosso del Cavaliere 100, 00133 Rome, Italy

Received 11 October 1999 / Accepted 14 March 2000

Abstract. The subject of this paper is the attempt to reproduce the CO observed production rate curve of comet Hale-Bopp with a numerical model of the nucleus thermal evolution and chemical differentiation. Three possible mechanisms can contribute to the total measured CO production: 1) sublimation of CO from the nucleus; 2) release of gas of CO trapped in the amorphous water ice in the nucleus; 3) emission of CO from grains in the inner coma (diffuse source). To match production rate observations with a numerical model we need an interplay between these emission mechanisms: success (and failure) in reproducing observed curve gives us useful information about the relative importance of these mechanisms and the depth of sublimation front. Using a numerical model of the nucleus we were able to match the observed CO production curve using quite standard initial parameters. We verified that it is impossible to reproduce the observed CO production curve taking solely into account sublimation of CO from ice contained in the nucleus or the release of gas of CO trapped in the amorphous water ice: if amorphous ice is not present immediately below the surface, we have to invoke some other physical process resulting in a perihelion CO production peak, such as a distributed source in the coma and/or the release of some of the trapped CO during water ice sublimation.

Key words: comets: individual: C/1995 O1 Hale-Bopp – comets: general

1. Introduction

The subject of this paper is the attempt to reproduce the observed CO production rate curve of comet Hale-Bopp with a numerical model of the nucleus thermal evolution and chemical differentiation. Due to the lack of direct data on cometary nuclei, these kind of models are useful to link observations, usually referring only to the coma, with real characteristics and properties of the nucleus. The coming of such an extraordinary comet as Hale-Bopp has given the unique (so far!) opportunity to observers of obtaining an unprecedented coverage of the activity of a comet passing through the inner Solar System, and to modellers of testing and comparing theoretical results with observational data.

There are three possible mechanisms that can contribute to the total measured CO production in a comet: 1) sublimation of the ice of CO from the nucleus; 2) release of gas of CO trapped in the amorphous water ice in the nucleus; 3) emission of CO from grains in the inner coma (distributed or extended source). Following experimental results (Bar-Nun & Owen 1998, Bar-Nun et al. 1985, Bar-Nun et al. 1987, Hudson & Donn 1991, Jenniskens & Blake 1994), trapped gases are emitted during the transition between the amorphous and crystalline phase of water ice. Moreover, it seems that some of this gas is released only at the moment of water ice sublimation. The possibility of a distributed source in the inner coma for CO and other volatiles was suggested many times for various comets (Meier et al. 1993, Samarasinha & Belton 1994), including Halley (Eberhardt et al. 1987) and Hale-Bopp (Di Santi et al. 1999). To match production rate observations with a numerical model we need an interplay between these emission mechanisms: success (and failure) in reproducing observed curve can give us useful information about the relative importance of these mechanisms and the origin of observed CO.

From the moment in which the unique opportunity offered by comet Hale-Bopp was clear, several papers about nucleus theoretical models applied to the foreseeing and interpretation of the activity of this comet were published. A direct comparison between different models (and ours) will not be attempted here, because of their widely different formulations, parameters and initial conditions. We will limit ourselves to a short description of the results of some of them.

Prialnik (1997) published their numerical results before the arrival of the comet at perihelion. Their model nucleus is made by amorphous water ice, dust and a fraction of 5 per cent in mass of gas of CO trapped in amorphous ice and released during the transition: in this model all emitted CO is coming from the release of trapped gas. They predict that CO emission, coming only from a subsurface layer, should not continue to rise until perihelion, and that should become quite flat.

Flammer et al. (1998), that published shortly after Hale-Bopp perihelion, used the model developed by Houpis et al. (1985). The nucleus is composed by a homogeneous grainy admixture of dust, H_2O-clathrate grains and grains of CO.

Send offprint requests to: M.T. Capria
Correspondence to: capria@ias.rm.cnr.it

"Guest" molecules of CO are trapped in the clathrate (5 per cent). The authors did consider the effect of preceding passages through the inner Solar System. They predict outgassing values slightly lower post-perihelion, and conclude that the production rate curve of the comet can be explained by the mantled nature of a chemically differentiated nucleus. Their CO production curve is flat. It should be noted, howewer, that no experimental evidence seems to exist for clathrate-hydrate formation under solar nebula conditions, except for methanol (Bar-Nun & Owen 1998).

In the two-dimensional model by Enzian et al. (1998) solid CO is assumed to be both trapped in amorphous water ice and as an independent ice phase. The authors obtain a good agreement with observations and moreover successfully explain high water production near 3 AU pre-perihelion with the sublimation from icy grains in the inner coma. Their simulation starts at 20 AU and considers only one perihelion passage.

We already applied our code to Hale-Bopp simulation, shortly after perihelion passage (Capria et al. 1997); two models were presented, one with CO coming from sublimation of nucleus ice and the other one with CO being released from amorphous ice during transition to crystalline form. From the results of these models we predicted two different trends for post-perihelion CO production curve, and concluded that it was impossible, with then available data, to determine if CO was coming mainly from independently sublimating ices or if it was being released by crystallization. Now that Hale-Bopp production curves are known until 8 AU post-perihelion we conclude this simulation and give our final conclusions. This time we consider also the possibility that, as seen in laboratory experiment on amorphous ices, some of the trapped gas could be released only at the time of water ice sublimation.

In the following paragraph the different CO emission mechanisms in comets will be discussed, and results of laboratory experiments on the behaviour of gases trapped in amorphous ice will be reviewed. In the third paragraph a short account of Hale-Bopp observations will be given; in the fourth paragraph the nucleus analytical model will be briefly described and model results will be presented and discussed in the fifth paragraph.

2. CO emission in comets

CO has been known for a long time as a parent cometary volatile, directly detected at ultraviolet wavelengths since 1983 (Feldman et al. 1983). It is the second most abundant constituent of comets, after water, with variable abundances (2–30 per cent relative to water, see for example recent measurements of Feldman et al. 1997); due to the very low sublimation temperature of 25 K (Yamamoto 1985), it dominates sublimation and is the driver of cometary activity at distances greater than 4–5 AU. CO observations are mainly done in EUV, due to the lack of a band system connected to the ground state in the optical region, and are difficult to perform and interpret.

CO is one of the molecules found to have also a distributed source (Meier et al. 1993, Samarasinha & Belton 1994, Eberhardt et al. 1987); the contribution of this distributed source to the total production rate is uncertain. Huntress et al. (1991) suggest that carbon suboxide could be responsible for the distributed source of CO, because this species, obtained in laboratory by ion irradiation by Brucato et al. (1997), is readily decomposed after being released from the nucleus. An extended source could explain the disagreement between UV and IR observations, mostly sensitive to parent CO, and radio observations, sensitive also to extended emission (Senay et al. 1996, Womack et al. 1996). Howewer, objections raised by Crifo & Rodionov (1999) to the "automatic interpretation" of some observations in terms of distributed source should be taken into account. For example, their opinion is that the increase in the CO and H_2O flux, observed in the results of the Giotto neutral mass spectrometer, is only apparent and due to the "unrealistic" assumption of a spherical nucleus. They do not exclude, however, that photodestruction of molecules can increase the relative abundance of CO in the coma.

2.1. The behaviour of amorphous ice

A possible emission mechanism for CO is the release from amorphous water ice. At low pressure and temperature (under 120 K) water ice occurs in a metastable state called amorphous ice (Jenniskens et al. 1998); this form can persist for timescales comparable to the lifetime of the Solar System, due to activation energy barriers preventing transition from a form to another. When warmed to about 150 K, amorphous ice transforms into a cubic crystalline form and then, under confinement pressure and at temperatures of 195–223 K, into the stable hexagonal crystalline form. Amorphous water ice has physical properties (density, thermal conductivity and so on) which are very different from those of crystalline state, and has the ability to trap molecules with low sublimation temperatures that are expelled during the crystallization process.

What we know about the physical properties of amorphous ice and its behaviour upon warming comes from laboratory experiments (Bar-Nun & Owen 1998, Hudson & Donn 1991, Bar-Nun et al. 1985, Bar-Nun et al. 1987, Jenniskens & Blake 1994).

In these experiments, water vapour and gases such as CO are codeposited at low temperatures, obtaining amorphous ice; once the gas is trapped, in an amount decreasing with the increase of deposition temperature, its release depends only on changes in the ice structure related to temperature changes. A major release occurs when ice transforms into cubic ice ($\sim 145\,K$); this release could be partly responsible for the distant activity of comets (Prialnik & Bar-Nun 1992, Prialnik 1992). Interestingly, some gas is held so tightly that it is released only when the ice sublimates.

3. Hale-Bopp from observations

The brightness of Hale-Bopp allowed to monitor its activity with many different instruments and in various spectral ranges from 7 AU pre-perihelion to, at the time of this writing, more than 8 AU post-perihelion: this comet is providing the widest observational coverage of cometary activity obtained so far. Already many

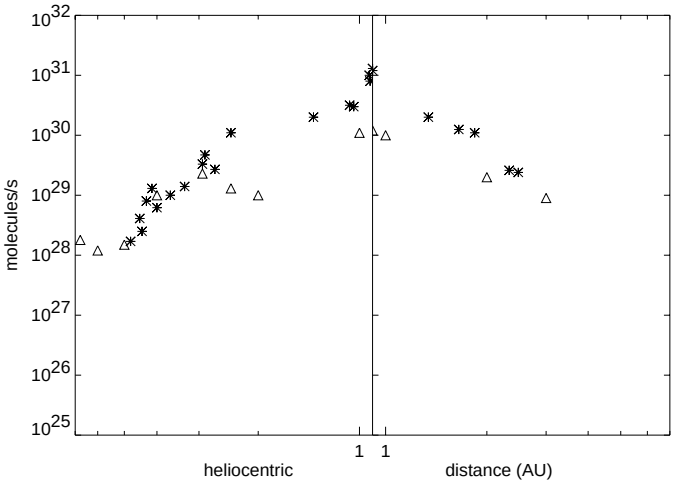

Fig. 1. OH (asterisks) and CO (triangles) from various published observations.

papers have been published on the results of the monitoring programs; besides the papers cited in the text, the reader could refer to review papers such as the one by Bockelée Morvan & Rickman (1999) and, in general, to all the papers presented at the First International Conference on comet Hale-Bopp held in Tenerife in 1998, and to more recent summary papers such as the one by Rauer (1999). Some of the results more relevant to the argument of this paper will be in the following shortly summarized.

The orbit of the comet changed noticeably from its first detection in 1995 to the perihelion passage (Bailey et al. 1996): due to the close encounter with Jupiter at an approach distance of 0.772 AU on 1996 April 5 TT, the semimajor axis reduced from 330 AU to 195.4 AU. As a consequence, the orbital period decreased from ~ 6000 to 2730 years, while the eccentricity remained quite the same (0.99722 pre-encounter, 0.99532 post-encounter).

As soon as it was discovered at 7.4 AU on July 23, 1995 (Hale & Bopp 1995), it was immediately clear that it was an exceptionally active comet. From the successive analysis of earlier images it seems that the comet was active already at about 13 AU and probably even farther, at 18–20 AU (Fitzsimmons 1999). CN was detected spectroscopically in the visible at 6.82 AU (Fitzsimmons & Cartwright 1996), CO was detected a few weeks later at 6.6 AU by millimetre spectroscopy (Jewitt et al. 1996, Biver et al. 1996) and OH at 4.8 AU by the HST (Weaver et al. 1997). In Fig. 1 production curves of OH and CO, taken from published observations with different techniques (Biver et al. 1999, Colom et al. 1999) are reproduced.

CO appears to be the driver of cometary activity until 4–3.5 AU, when water sublimation becomes dominant. A steep increase in CO (and other minor volatiles) production can be noticed near 4.8 AU, in coincidence with the first detection of OH. While before perihelion the transition between CO-driven activity and H_2O-driven activity occurred at 3.4 AU, after perihelion the transition occurred at 2–2.5 AU (Colwell et al. 1999).

Crovisier et al. (1997) deduced, from the ortho/para ratio (OPR) of water, a formation temperature of about 25 K and no subsequent re-equilibration. They also detected crystalline olivine (forsterite). Analyzing pre-perihelion observations, Weaver et al. (1997) observe that water is not the driver of dust production before 4 AU because the heliocentric distance dependence of dust production is different from that of H_2O production. They also suggest that water production values at greater heliocentric distances could be explained by sublimation from icy grains or ice coated dust grains. The authors constrain the diameter of the nucleus between 27 km and 42 km. The signature of icy grains was detected near 6 AU and 3 AU (Davies et al. 1997, Leech et al. 1999). The presence of a halo of icy grains, maybe releasing also minor volatiles, is further suggested by the near constancy of $Af\rho$ between 4.6 and 2.4 AU (Rauer et al. 1997), contrasting with increasing gaseous activity. Biver et al. (1997) suggest, from radio observations, that CO should be released mainly by the nucleus and that sublimating icy grains were still present in the coma at 3.5 AU. Di Santi et al. (1999) found that H_2CO could be an extended source for an important fraction of CO. Rauer (1999) observes that the comet seems not to be old and highly differentiated, because CO (and minor volatiles in general) sublimation responds to varying solar input and this is not expected from the deep sublimation fronts of a differentiated comet. Anyway Hale-Bopp, having a nearly equal production of C_2 and CN, is considered to have a "typical" composition (A'Hearn et al. 1995), common to most of long period comets.

To conclude, the following points are particularly interesting from the point of view of nucleus modellers: 1) the production rate of CO and other minor volatiles seems to increase with the beginning of water sublimation; 2) CO emission is peaked with water at perihelion; 3) CO production is high also between 7 and 6 AU pre- (and post-) perihelion; 4) water production seems to start quite far from the Sun, when it cannot be explained by sublimation from the surface.

4. Nucleus model and initial assumptions

A short description of the nucleus model, along with a list of the physical processes which it accounts for (listed in Table 1), will be given in the following; for more details the reader is referred to Capria et al. (1996), Coradini et al. (1997), De Sanctis et al. (1999). A different implementation of the same model exists (Orosei et al. 1999) and is being maintained also for testing purposes.

The model is uni-dimensional. The spherical nucleus, porous and initially homogeneous, is composed by ices (water and CO, in this application) and a refractory component; a fraction of CO can be trapped in the amorphous matrix and released during the transition to crystalline phase. The refractory material is described as spherical grains with given initial size distribution and physical properties. Up to two grain populations with different physical properties and size distributions can be considered in the model. Energy and mass conservation is ex-

pressed by the following system of coupled equations, solved for the whole nucleus:

$$\rho c \frac{\partial T}{\partial t} = \nabla[k \cdot \nabla T] + \sum_{i=1}^{n} Q_i + Q_{am-cr}$$

$$\frac{1}{RT}\frac{\partial P_i}{\partial t} = \nabla[G_i \cdot \nabla P_i] + Q\prime_i \;\; i = 1, n$$

where Q_i are the energies exchanged by the solid matrix in the sublimation and recondensation of the ices, Q_{am-cr} is the heat released during the transition of water ice from amorphous to crystalline form, R is the gas constant, P_i the partial pressure of component i, G_i its diffusion coefficient, and $Q\prime_i$ is the gas source term due to sublimation-recondensation processes. In the case of the CO diffusion equation, the gas source term due to the release of trapped CO, $Q_{CO_{tr}}$, must be added. We assume, as done by Tancredi et al. (1994) and Prialnik (1997), that the energy consumed in the release of CO is negligible compared to the energy released during the phase transition, which consequently is not reduced.

Thermal conductivity of the bulk material is computed by means of Russel's formula:

$$k = \frac{k_s[\psi^{2/3}k_p + (1-\psi^{2/3})k_s]}{k_s[\psi - \psi^{2/3} + 1] - k_p\psi^{2/3}[\psi^{1/3} - 1]}$$

where ψ is the porosity, k_s is the conductivity of the solid phase and k_p is the effective conductivity due to radiative energy transfer across the pores (expressed as $4\epsilon\sigma r_p T^3$, ϵ being the thermal emissivity, σ the Stefan-Boltzmann constant and r_p the mean pore radius).

Gas diffusion coefficients are computed on the basis of the mean free path of the molecules in the pore system; the model accounts for three different diffusion regimes: Knudsen, viscous and a transition one. It can be noted that in usual conditions diffusion regime is Knudsen's, so we can assume that each gas flows independently from the others.

Nucleus rotation effects can be taken into account: the model can be run both in the fast rotator approximation (the incoming energy can be assumed to be uniformly distributed along a thin belt at a given latitude), and in the slow rotator approximation (by allowing the variation of solar illumination due to the rotation of the nucleus).

The temperature on the surface is obtained by a balance between the solar energy reaching the surface, the energy reemitted in the infrared, the heat conducted to the interior and the energy used to sublimate surface ices. Due to the rising temperature, ices start to sublimate, beginning from the more volatile ones, and the initially homogeneous nucleus differentiates giving rise to a layered structure in which the boundary between different layers is a sublimation front.

When the ices near the surface of the nucleus begin to sublimate, the refractory particles become free and undergo the drag exerted by the escaping gas, so that they can be blown off or they can accumulate on the surface to form a crust. To determine how many particles can be blown off and how many can be accumulated on the surface, the different forces acting on the single grain are compared, obtaining for each distribution a critical radius that represents the radius of the largest particle that can leave the comet. Surface erosion due to ice sublimation, particles ejection and crust compaction is computed at each step.

Table 1. Phenomena accounted for in the model

heat conduction by the solid phase
heat transport (advection) by the vapour phase
gas diffusion in a porous medium
sublimation of volatiles in the nucleus
gas fluxes from the surface
recondensation of volatiles in the nucleus
amorphous-crystalline transition
release of gases trapped in the amorphous ice
surface erosion (radius reduction)
crust formation
crust ablation
dust flux from the surface
nucleus rotation (day/night effects)
axis obliquity effects

Table 2. Initial parameters of the model

albedo	0.04
porosity	0.8
emissivity	0.96
dust/ice	1
dust density	1000 $kg\ m^{-3}$
dust conductivity	3 $W\ m^{-1}K^{-1}$
initial temperature	20 K
initial pore radius	$10^{-5}m$
rotation period	11.4 hrs
initial radius	20 km

Such a model depends on many parameters describing the orbit, the initial conditions of the nucleus and its physical properties. In Table 2 some of our assumptions are shown. The parameters shown here were never changed in the cases we are going to present and are quite typical in nucleus modeling: we chose, for this work, to concentrate only on CO behaviour and varied only parameters concerning CO (such as the amount of CO trapped in amorphous ice).

The ice is always initially amorphous, as it should be if formed at the temperatures suggested by the OPR of water (Crovisier et al. 1997). Weaver et al. (1997) suggested, from the analysis of HST images, that the diameter of Hale-Bopp should be constrained between 27 and 42 km, and these values were later confirmed: we adopted a value of 20 km for the radius. The rotation period is taken from Samarasinha et al. (1999). The conductivity of crystalline ice is given by 567/T $W\ K^{-1}\ m^{-1}$ (Klinger 1980). For the conductivity of amorphous ice we assumed, due to the present uncertainty between the theoretical estimate given by Klinger (1980) and the much lower values found by Kouchi (1992), an intermediate value of 7.1 $10^{-7}\ T\ W\ m^{-1}\ K^{-1}$ (see for example Tancredi et al. 1994). The resulting bulk conductivity of cometary material is comprised between 0.1 and 0.2 $W\ m^{-1}\ K^{-1}$, and average density is 200 $kg\ m^{-3}$.

In order to reproduce the dynamical evolution of the body (Bailey et al. 1996), we started our computations at the aphelion of the pre-Jupiter-encounter orbit (semimajor axis = 330 AU, eccentricity = 0.997223); then, after a couple of revolutions, we moved on the new orbit (semimajor axis = 195.4 AU, eccentricity = 0.99532) from an arbitrarily chosen point near 4.5 AU. In this way we are simulating the fact that this comet was not dynamically new, and that the upper layers should have been more or less differentiated, until a depth depending on nucleus properties.

5. Discussion of results

Case 1 – The simplest hypothesis: only sublimation from ice

We start from the simplest hypothesis (hereafter case 1): the nucleus is composed by dust and a mixture of ices of water and CO; ice is initially amorphous but no gas is trapped inside; all the ices are sublimating at their sublimation fronts. The initial amount of CO is 5 per cent with respect to water.

When we start the computation the comet is very far from the Sun and for a long time (thousands of years!) nothing happens: all the activity and the consequent mass loss are concentrated in a span of years really short with respect to the orbital period. This concentrated activity is coupled with a strong erosion that keeps sublimation and transition fronts close to the surface. These considerations apply to both the orbits considered (pre- and post-Jupiter encounter) and apply also to long period comets in general, due to the highly elliptic shape of their orbits. The effect of previous perihelion passages is that, when the comet arrives on the present orbit, the first few metres under the surface are differentiated and evolved, that means depleted from more volatile gases and with the ice in crystalline phase: CO sublimation front can be found well under the surface. Anyway, it should be noted that surface sublimation of CO ice is ruled out by the sublimation temperature of this ice, and by the fact that the expansion velocity of $0.5\ km\ s^{-1}$ measured at large distance in the coma (Biver et al. 1997, Jewitt et al. 1996) is well explained by a subsurface sublimation and diffusion through a hotter sublimation-free surface.

The production rate curve of CO obtained with this model is shown in Fig. 2, along with data from observations. In this plot, like in the following ones, the production rate represents an upper limit: the whole surface is considered active and emitting like at the equator.

Activity starts very far from perihelion because CO is a very volatile gas, sublimating under 30 K: at 20 AU pre-perihelion the CO flux is already of the order of $10^{27}\ molec\ s^{-1}$. Its sublimation front, that was about ten metres from the surface at the aphelion of preceding orbit, remains in a layer of quasi-constant temperature, even considering surface erosion, and can be reached by thermal wave with a delay depending on its depth. The curve tends to assume a flat appearance for a long time span: we obtain a "flat" production curve, with a small peak after perihelion, when heat wave reaches the sublimation front. Changing the initial amount of CO or bulk conductivity or the differentiation state of first layers cannot change the shape of the curve, but only move it up and down: with these initial assumptions we can explain distant activity but we cannot match in any way near-perihelion observations and obtain a perihelion production peak.

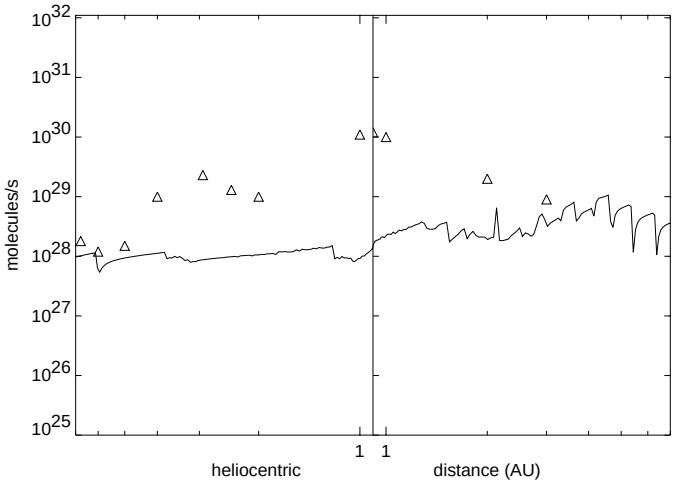

Fig. 2. Case 1: CO production rate from model (continuous line) and observations (triangles).

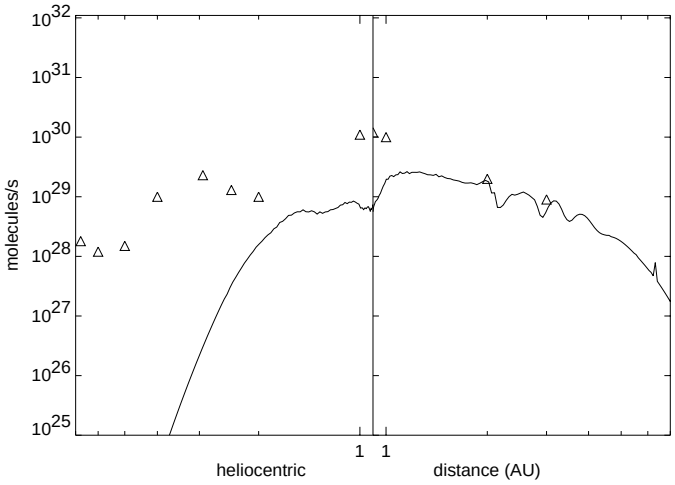

Fig. 3. Case 2: CO production rate from model (continuous line) and observations (triangles).

Case 2 – All the CO is contained in the amorphous ice

In the second case we are assuming that all the CO is initially contained as a trapped gas in the amorphous ice. The initial amount of CO is 10 per cent of the mass of amorphous ice, and this amount is all released during transition to the crystalline phase. This transition is occurring in layers with a temperature much higher than CO ice sublimation temperature, between 130 and 145 K, and consequently the gas is coming from layers much closer to the surface than in case 1 (how much nearer will be discussed in the following). What was written about the simulation of nucleus ageing applies also to this case and to the following ones. CO production rate curve is shown in Fig. 3.

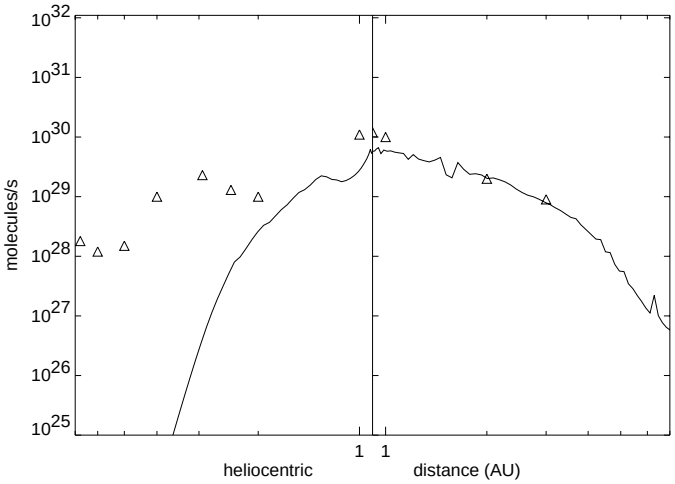

Fig. 4. Case 3: CO production rate from model (continuous line) and observations (triangles).

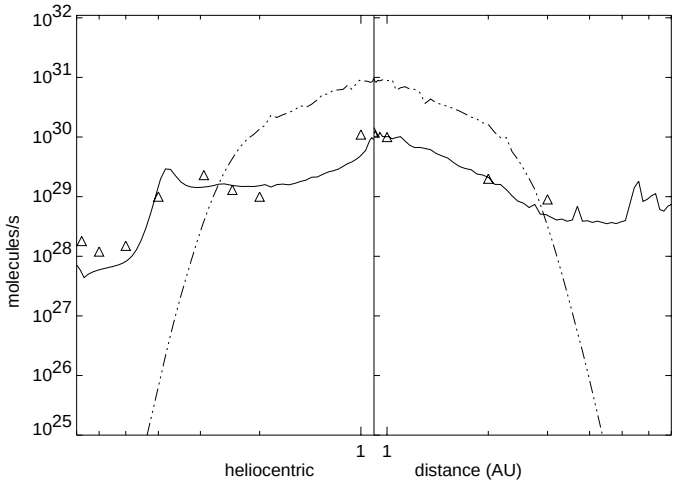

Fig. 5. Case 4: production rates of CO (continuous line) and H_2O (dashed line) from model, and of CO (triangles) from observations.

With the initial assumptions of this case we cannot explain any kind of activity far from the Sun, when internal temperatures do not allow phase transition and the consequent gas release. Anyway, observing the shape of the curve, that is no more flat, it should be noticed that we could obtain a production peak at perihelion if we suppose that amorphous ice can be found very close to the surface: the position of the CO production peak depends, in this case, on the time at which the heat wave reaches the layer containing amorphous ice, and this time, in turn, depends on the depth of transition front. Changing some of the initial conditions (for example, strongly lowering thermal conductivity or assuming that the transition is not exothermic) we could probably obtain such a peak; the feasibility of finding the transition front immediately under the surface will be discussed in the following.

Case 3 – What if some of trapped CO is released as water sublimates?

Now let us suppose, for the third case, that not all the trapped CO is released during phase transition, but that some (up to half of the total) is released only during water ice sublimation; all other initial assumptions are the same as for case 2. This phenomenon, observed in laboratory experiments, could be (see also Bockelée-Morvan & Rickman et al. 1999, Rauer 1999) a good explanation, alternative to that of the distributed source, for the fact that the production rates of many minor volatiles seem to increase with the beginning of water sublimation. The production curve of CO obtained with these assumptions is shown in Fig. 4.

In this hypothesis it is always possible to obtain a production peak at perihelion, even if the front of amorphous-crystalline transition is well under the surface; more or less matching near perihelion observations is a matter of choosing the "right" amount of total CO and of CO fraction emitted with H_2O. Howewer we stress once more, at this point, that a perihelion peak in CO emission (and, in general, a strong near-perihelion rise) could be obtained also by supposing minor volatile emission from grains in the inner coma, the so called distributed source; only a careful analysis of the results of observations can favour one or another of the two hypotheses.

Case 4 – The "right" one

It should be clear, at this point, that the right "recipe" to match observations without assuming some kind of source in the inner coma is put together the cases 1, to explain distant activity, and 3, to have a perihelion peak. The obtained CO production curve is shown in Fig. 5, along with that of H_2O, shown only here because it is essentially the same in all the preceding models.

In case 4 we are assuming that the nucleus is composed by dust and ices of H_2O and CO (4 per cent with respect to water), and by CO trapped as a gas in the amorphous ice (10 per cent in mass). Given the probable formation temperature of the comet, and its orbit, it is well possible that CO can be found both as an ice and as a trapped gas. We are also supposing that some of the trapped gas (say, 20 per cent of the total) is being released only with water sublimation. In this way, using quite standard parameter values and laboratory results, we can reproduce (and consequently interpret) the observed CO production curve in Hale-Bopp. Note that we do not reproduce water sublimation between 3 and 4 AU: we agree with Enzian et al. (1998) that it should be needed to introduce water sublimation from grains in the inner coma, as they did and as was confirmed by observations. Dust production rate is, at perihelion in this and in preceding cases, of the order of $10^6 - 10^7 kg\ s^{-1}$, in agreement with the observations (see, for example, Jewitt et al. 1996).

It remains to discuss the depth of transition front and erosion effects in general. In Fig. 6 a stratigraphy plot is shown; it is similar for all the preceding cases and shows the layering of nucleus at the last perihelion passage for case 4.

It can be noticed that, after few orbits, transition front stabilizes at a depth of few metres and that, at each perihelion passage, many metres of surface are lost: the comet is in some

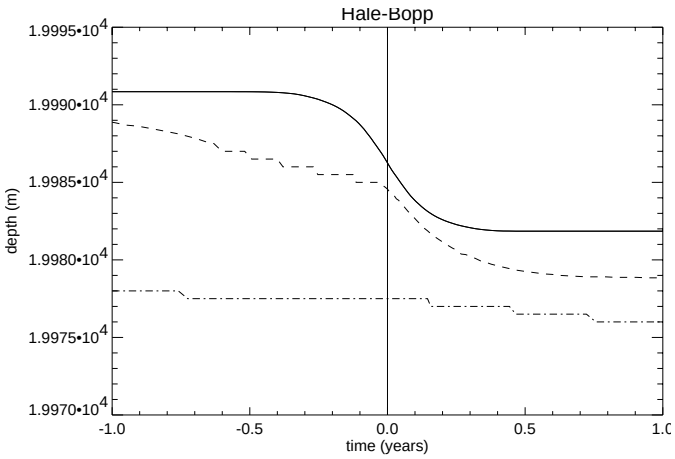

Fig. 6. Stratigraphy of the nucleus during two years before and after the last perihelion passage (case 4). The time of perihelion is marked by a vertical line.

way rejuvenated at each passage, so there is no reason to suppose that it is dynamically new to explain why this body seems to be not deeply differentiated. In the computed stratigraphy, amorphous ice is found neither immediately below the surface nor very far. It should be mentioned that close encounters with giant planets do not really modify perihelion distance, a fundamental parameter in determining activity and, consequently, erosion.

What if dust/ice ratio in the nucleus would be much higher than 1, as suggested by Jewitt et al. (1996) on the basis of their observations? We think that this should not affect qualitatively our results. Higher refractory content usually results in a higher bulk conductivity, which means that sublimation and transition fronts should be deeper, and dust flux higher.

6. Conclusions

Using a numerical model of nucleus thermal evolution and chemical differentiation we were able to qualitatively reproduce observed CO production curve using quite standard parameters and initial assumptions. We verified that it is impossible to reproduce measured values only by letting CO sublimate as an independent ice phase, or only by allowing CO release during transition from amorphous to crystalline ice phase. We need both mechanisms to explain long distance activity and near perihelion surge. If amorphous ice cannot be found immediately below the surface, as we consider more probable, we have to introduce a physical process resulting in a perihelion production peak, such as a distributed source for CO and/or the release of some of the trapped CO during water ice sublimation, as seen in laboratory experiments. We conclude, moreover, that there is no need to suppose that the comet is dynamically new to explain why it does not seem to be very differentiated, because during each perihelion passage many metres of surface are lost, and sublimation and transition fronts can always be found few metres below the surface.

References

A'Hearn M.F., Millis R.L., Schleicher D.G., Osip D.J., Birch P.V., 1995, Icarus 118, 223
Bailey M.E., Emel'yanenko V.V., Hahn G., et al., 1996, MNRAS 281, 916
Bar-Nun A., Herman G., Laufer D., Rappaport M.L., 1985, Icarus 63, 317
Bar-Nun A., Dror J., Kochavi E., Laufer D., 1987, Phys. Rev. B 38, 7749
Bar-Nun A., Owen T., 1998, In: Schmitt B., et al. (eds.) Solar System Ices. p. 139
Biver N., Rauer H., Despois D., 1996, Nat 380, 137
Biver N., Bockelée-Morvan D., Colom P., et al., 1997, Sci 275, 1915
Biver N., Bockelée-Morvan D., Colom P., et al., 1999, Earth Moon Planets, in press
Bockelée-Morvan D., Rickman H., 1999, Earth Moon Planets 79, 55
Brucato J., Castorina A.C., Satorre M.A., Strazzulla G., 1997, Planet. Space Sci. 45, 835
Capria M.T., Coradini A., De Sanctis M.C., 1997, In: IAU XXIII, Special Session on Comet Hale-Bopp, p. 9
Capria M.T., Capaccioni F., Coradini A., et al., 1996, Planet. Space Sci. 44, 987
Colom P., Gerard E., Crovisier J., et al., 1999, Earth Moon Planets, in press
Colwell W.B., Festou M.C., Stern S.A., et al., 1999, LPI, 1153
Coradini A., Capaccioni F., Capria M.T., et al., 1997, Icarus 129, 317
Crifo J.F., Rodionov A.V., 1999, Planet. Space Sci. 47, 797
Crovisier J., Leech K., Bockelée-Morvan D., et al., 1997, Sci 275, 1904
Davies J.K., Roush T.L., Cruikshank D.P., et al., 1997, Icarus 127, 238
De Sanctis M.C., Capria M.T., Capaccioni F., et al., 1999, Planet. Space Sci. 47, 855
Di Santi M.A., Mumma M.J., Dello Russo N., et al., 1999, Earth Moon Planets, in press
Eberhardt P., Krankowsky D., Schulte W., et al., 1987, A&A 187, 481
Enzian A., Cabot H., Klinger J., 1998, Planet. Space Sci. 46, 851
Feldman P.D., 1983, Sci 219, 347
Feldman P.D., Festou M.C., Tozzi G.P., Weaver H.A., 1997, ApJ 475, 829
Fitzsimmons A., Cartwright I.M., 1996, MNRAS 278, L37
Fitzsimmons A., 1999, Earth Moon Planets, in press
Flammer K.R., Mendis D.A., Houpis H.L.F., 1998, ApJ 494, 822
Hale A., Bopp T., 1995, IAU Circ. 6187, 1995
Huntress W.T., Allen M., Delitsky M., 1991, Nat 352, 316
Houpis H.L.F., Ip W.H., Mendis D.A., 1985, ApJ 295, 654
Hudson R.L., Donn B., 1991, Icarus 94, 326
Jenniskens P., Blake D.F., 1994, Sci 265, 753
Jenniskens P., Blake D.F., Kouchi A., 1998, In: Schmitt B., et al. (eds.) Solar System Ices. p. 139
Jewitt D., Senay M., Matthews H., 1996, Sci 271, 1110
Klinger J., 1980, Sci 209, 271
Kouchi A., Greenberg J.M., Yamamoto T., Mukai T., 1992, ApJ 388, L73
Leech K., Crovisier J., Bockelée-Morvan D., 1999, Earth Moon Planets, in press
Meier R., Eberhardt P., Krankowsky D., Hodges R.R., 1993, A&A 277, 677
Orosei R., Capaccioni F., Capria M.T., et al., 1999, Planet. Space Sci. 47, 839
Prialnik D., Bar-Nun A., 1992, A&A 258, L9
Prialnik D., 1992, ApJ 388, 196
Prialnik D., (1997) ApJ 478, L107

Rauer H., Arpigny C., Boehnhardt H., et al., Sci 275, 1909
Rauer H., 1999, In: A'Hearn M.F. (ed.) IAU Coll. 168, Cometary nuclei in space and time, in press
Samarasinha N.H., Belton M.J.S., 1994, Icarus 108, 103
Samarasinha N.H., Mueller B.E.A., Belton M.J.S., 1999, Earth Moon Planets 77, 189
Senay M., Matthews H., Jewitt D., 1996, IAUC 6335
Tancredi G., Rickman H., Greenberg J.M., 1994, A&A 286, 659
Yamamoto T., 1985, A&A 142, 31
Weaver H.A., Feldman P.D., A'Hearn M.F., et al., 1997, Sci 275, 1900
Womack M., Festou M.C., Stern S.A., 1996, IAUC 6345